Providing a control method of BTB-VSC converters under unbalanced faults

Mostafa Abbasi, Mehdi Nafar, Mohsen Simab
Department of Electrical Engineering, Marvdasht Branch, Islamic Azad University, Marvdasht, Iran

Article Info	ABSTRACT
	Microgrids need control strategies to achieve maximum performance. An appropriate control strategy should have high performance in unbalanced conditions in addition to normal conditions. Today, the use of microgrids, with a variety of power sources, including solar, wind, diesel, energy storage sources to increase the capability of distribution grid has made significant progress. However, controlling and managing their energy in the event of a fault is a challenge that researchers are faced. In this article, two microgrids connected to the grid are studied using a back-to-back (BTB)-voltage source converters (VSC) converter. The results of this research showed that by the usage of above-mentioned convertor first, with power management between microgrids the frequency remains constant in island mode second, they are isolated from each other in terms of faults. The results showed that the use of the proposed method controlled the frequency of two microgrids simultaneously.

Corresponding Author:

Mehdi Nafar
Department of Electrical engineering, Marvdasht Branch, Islamic Azad University, Marvdasht, Iran
Email: mnafar@miau.ac.ir

NOMENCLATURE

I	: Source current	P, Q	: Active, reactive power inputs
L, R	: Phase reactor inductance and resistance	Vd, Id, Pd	: DC side voltage, current, power
C	: DC side capacitance	d, q	: Synchronous d–q axis
ω	: Source voltage angular frequency	p, n	: Positive, negative components
m	: Modulation index		

1. INTRODUCTION

Microgrids (MGs) typically operate in grid-connected modes. In this situation, the frequency and voltage of the MGs have a certain value [1], [2]. Most of the distributed generation sources are connected to the grid by electronic power converters. Therefore, the technical and operational characteristics of MGs distinguish them from traditional one [3]. These differences provide the basis for research to improve microgrids [4], [5]. Some studies examine previous research on MGs by the US, Europe, Japan, and Canada, and various central and local control strategies for power-sharing in MGs [6]−[10]. A multi-generational control unit management strategy with drop-off features for active power control in the island state and a new approach for controlling the available charge energy due to the limitations of storage devices [11]. In addition, the precise performance of the drop-off strategy approach on the stability of the MG frequency with the wind turbines was studied in [12]. According to [13] highlights the role of electronics in MGs, especially inverter

voltage sources. It also introduces a proven and proven way to manage and control MGs. An MG network operates in one of the following cases [14]: i) if power is generated in the MG Be less than the required power, the original grid shall compensate for the power shortage; and ii) if the generating power exceeds the load, the surplus power is injected into the original grid.

Two main control architectures for frequency restoration (FR) are the centralized/distributed coordinate and decentralized. The former requires a communication network to support the necessary interaction between DGS. Some routine centralized/distributed coordinate control methods for DG were proposed in the literature [15]–[24], which include the consensus synchronization control through the state feedback control [22]–[24], the distributed cooperative adaptive control [18], [20], the centralized proportional-integral (PI) compensation control [21]–[23], and the synchronization signal injection control [24].

Depending on the operating conditions mentioned, the adjacent network can cooperate during fault conditions to maintain production and consumption in equilibrium. Therefore, gride network performance improves in an island state using optimum control strategies. Improved dynamic performance of two microgrids has been studied and evaluated. It seems that a significant improvement has been achieved compared to a single operation [25]. A single phase inverter transducer equipped with low voltage ride-through (LVRT) is controlled using the classic PI controller. The results indicate the effective participation of LVRT in the voltage profile control and improvement system but the system does not have a rapid response during LVRT [26]. It is obvious that the voltage drop caused by the fault is very fast and short and the control system must respond to these changes very quickly and operate promptly in the LVRT state. Wind turbine-based power plants have to remain in the grid for a specified period based on the voltage drop level created at the terminal or common connection point (PCC) [27]. Many solutions have been proposed using power electronics to control the current in electrical systems [28]. The use of back-to-back (BTB)-voltage source converters (VSC) converter is increasing due to the ability to control the current and the possibility of fast and independent control of active and reactive power [29].

Rosero *et al.* [30] specifies how to allocate active power and adjust frequency points. Drop control is used for AC MGs and power allocation, followed by frequency adjustment by replacing the secondary control and the primary drop mechanism to execute the MGcontrol strategy. Stability analysis in the power system has also been considered to investigate the sustained conditions in the system. Zhang *et al.* [31], several MGs are connected to the main network using a converter. The frequency control of these MGs is based on drop control. The outputs of these converters are connected by lines with Z impedance. These lines are of DC type but the MGs themselves are of AC type. Both AC and DC power are transferable. The drop control scheme is generally used in parallel with several inverters [32] in which the voltage and frequency of each inverter are adjusted to control the active and reactive power. A review of previous studies shows that most research is designed to study control strategies for single MGs. However, the issue of control strategies for two MGs that can play a supportive role is still neglected. Also, most strategies developed for normal conditions so fewer studies cover unbalance conditions. Therefore, in this research, a new method has been proposed to control two MGs connected to the grid in unbalanced condition error with a supportive role.

2. MODELING THE PROBLEM

MGs are recognized as low-voltage radial distribution networks. Depending on the available fuel type, numerous types of controllable diesel generator sources, micro-turbine, and fuel cell utilized in MG sources despite uncontrolled sources of a wind turbine, and photovoltaic. Ganthia *et al.* [2] compares and tests several empirical MG networks introduced in the literature. In this study, the MG presented in Luna *et al.* [12] to evaluate and correct the performance of the expressed method for frequency control using some frequent changes in the sources has been produced. The single-line diagram of the test system in Figure 1, shows that each MG is connected to the original network by a static switch, including loads, controllable and uncontrollable sources devices. All power sources are connected to the grid via both converter interfaces. In normal mode, two grids are connected to the network, so if an error occurs in the network each MG will be separated from the original network using switches 1 and 2. For this reason, they will continue to work in island mode. In fact, these MGs play a supporting role for each other. When a MG fails, the second MG seeks to support network load supply. The analysis of the connection of two MGs through a back-to-back voltage source converter (BTB) with local control is the main hypothesis and the main purpose of this paper. A BTB converter is required to control a dual-feed induction system because in some operating ranges the rotor energy may return to the converter. This converter has two parts on the side of the network and the side of the machine. Due to requiring energy return to the network, the direct voltage uses the internal current control loop so it provides a good permanent and transient response for the converter. The induction machine control is performed using the indirect vector control method. The BTB-VSC converter with the mentioned method both exchanges the specified power in island mode and helps both MGs to support each other for frequency control.
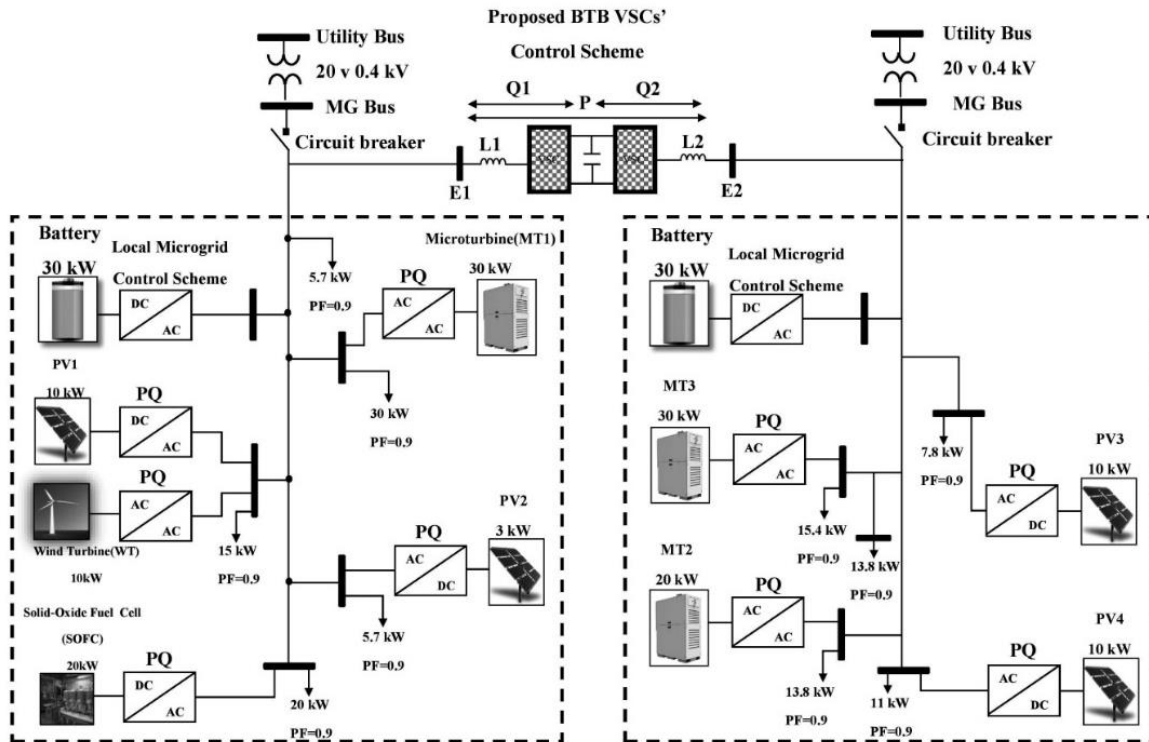
Figure 1. The structure of the MG and their connection through a back-to-back voltage source converter

3.   A REVIEW ON THE STRUCTURE OF BTB-VSC AND ITS MATH MODEL

In the sequel an overview of the BTB-VSC structure and its math model presented. Each BTB-VSC converter consists of two VSC and one bus with DC voltage. In order words two VSC are connected through a shared DC bus by means of which the work of both VSC are controlled independently. In what follows its structure and mathematical model have been examined in details.

3.1. A review on the structure of BTB-VSC

The BTB-VSC converter consists of two VSCs connected by a common DC bus voltage that allows the VSCs to be controlled separately. Both VSCs can act independently as rectifiers or inverters. The most common use of BTB-VSC converter is to balance and balance the active power, in other words, to adjust the active power between two sources connected to the grid. For the supplement of a single power factor on each side of AC grid a BTBVSC is used or as an inverter is responsible for providing a set AC output. It also provide the possibility of the control of the active and reactive powers of interconnected AC-AC systems. Meanwhile it allows the control of the active and reactive powers of interconnected AC-AC systems. VSC1 and VSC2 can act as rectifiers or inverters depending on the power direction. Active power can flow in both directions ($0 \leq |P|$). In addition, the BTB-VSC converter can operate with lagging power factor ($Q>0$) or leading power factor ($Q<0$).

3.2. The math model of BTB-VSC

The overall structure of the back-to-back voltage source converter is illustrated in Figure 2, the MG phase voltage and VSC converter output voltage, respectively, are shown in Figure 1. The intended BTB-VSC converters must be capable of transmitting a specified amount of P and Q power between E1 and E2 jacks. The "d-q" conversion is utilized to control the transmitted power. The d-q axis voltages are determined by converting the three-phase voltage and current of both sides of the BTB-VSC to a d-q reference that rotates at an angular velocity coordinate with E1,2. In the following relation, V 1, 2 indicates the AC voltage on both sides of BTB-VSC and Vd represents the voltage across the two sides of the BTB-VSC, corresponding to the d-axis and Vq represents the voltage across the two sides of the BTB-VSC, corresponding to the q-axis. I 1, 2 indicates the AC current on both sides of BTB-VSC and Id represents the current across the two sides of the BTB-VSC, corresponding to the d-axis and Iq represents the current across the two sides of the BTB-VSC, corresponding to the q-axis.

$$V_{d1,2} = E_{d1,2} + R_{1,2}i_{d_{1,2}} + L_{1,2}\frac{di_{d_{1,2}}}{dt} - \omega L_{1,2}i_{q_{1,2}} \tag{1}$$

$$V_{q1,2} = E_{q1,2} + R_{1,2}i_{q1,_2} + L_{1,2}\frac{di_{q_{1,2}}}{dt} - \omega L_{1,2}i_{d_{1,2}} \tag{2}$$

Where in:

$$E_{q1,2} = 0 \tag{3}$$

$$E_{d1,2} = E_{1,2} \tag{4}$$

The q-d currents are expressed as voltage disturbances separately in (5) and (6). To clarify all equations subscripts 1 and 2 related to VSC$_1$ and VSC$_2$, respectively. i1, 2 and v1, 2 are the currents and voltages of the AC source and the load; ω (ω=2 Πf), R1, 2 and L1, 2 are the resistance and the inductance of the line(s) used to interconnect the BTB converter to the AC system(s). The equivalent circuit is obtained from Figure 2 by placing the number of voltages at the input and output terminals of VSC1 and VSC2 with controlled voltage sources and the amount of DC currents with controlled current sources, as shown in Figures 3 and 4. The controller model is shown in Figure 3. Includes multiplication of control inputs and mode variables and reciprocal pair conditions between DQ components. The d-axis is selected along the AC sources v1 and v2, respectively, so V1, 2d is equal to the corresponding AC source amplitude and V1, 2q are zero.

$$V'_{d1,2} = R_{1,2}i_{d_{1,2}} + L_{1,2}\frac{di_{d_{1,2}}}{dt} \tag{5}$$

$$V'_{q1,2} = R_{1,2}i_{q_{1,2}} + L_{1,2}\frac{di_{q_{1,2}}}{dt} \tag{6}$$
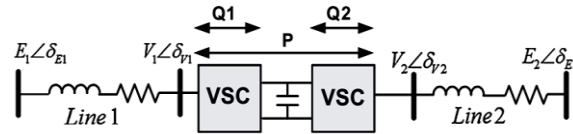

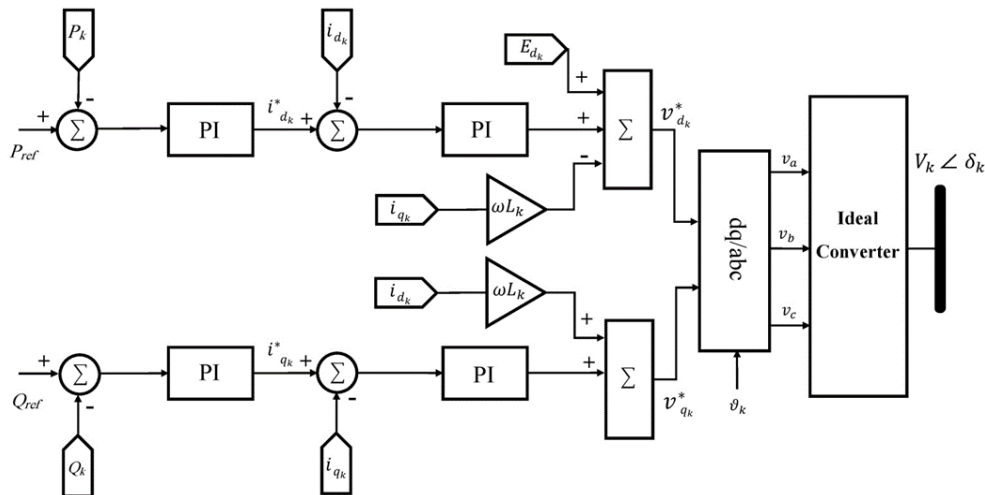Figure 2. The overall structure of the BTB-VSC converter

Figure 3. PQ controller structure (K=1 or K=2)

According to (5) and (6), the changes in the current i$_q$ and id contribute to the same-axis voltage changes through the first-order differential equations. A suitable integrated controller is provided, which can generate references for current and voltage. For example, for VSC2 we have:

$$V'_{d2} = \left(K_{pd2} + \frac{K_{Id2}}{s}\right) \cdot (i^*_{d2} - i_{d2}) \tag{7}$$

$$V'_{q2} = \left(K_{pq2} + \frac{K_{Iq2}}{s}\right) \cdot (i^*_{q2} - i_{q2}) \tag{8}$$

Kpd2 and Kpq2, Kid2 and Kiq 2 represent the coefficients of the PI controller, corresponding to the d and q axes for VSC2. By combining the previous equation, we will have:

$$V^*_{d2} = E_{d2} + \left(K_{pd2} + \frac{K_{Id2}}{s}\right) \cdot (i^*_{d2} - i_{d2}) - \omega L_2 i_{q_2} \tag{9}$$

$$V^*_{q2} = E_{q2} + \left(K_{pq2} + \frac{K_{Iq2}}{s}\right) \cdot (i^*_{q2} - i_{q2}) - \omega L_2 i_{d_2} \tag{10}$$

Vd and Vq is the reference voltage corresponding to the d-axis and the q-axis.

To manage active and reactive power due to the converter losses, the active and reactive power produced by the converter can be generated by (11) and (12).

$$P_2 = \frac{3}{2}\left(V_{d2} i_{d2} + V_{q2} i_{q2}\right) = \frac{3}{2} V_{d2} i_{d2} \tag{11}$$

$$Q_2 = \frac{3}{2}\left(V_{q2} i_{q2} - V_{d2} i_{d2}\right) = -\frac{3}{2} V_{d2} i_{q2} \tag{12}$$

Figure 3 shows the power control block diagrams as well as the internal and external control loops. The external control loop represents the current reference and the internal control loop represents the voltage reference based on the d-q axis. Figure 4 shows the control diagram of the BTB-VSC converter, which has a transmission power based on two MG frequencies. Here the task of controlling the amount of DC-link voltage is assigned to VSC1 and VSC2 is used to control the active power. Reactive power adjustment is achieved using the corresponding VSC on the output side. The variables and parameters to be controlled here are: vdc and Q1 to VSC1, while P2 and Q2 are controlled by VSC2.
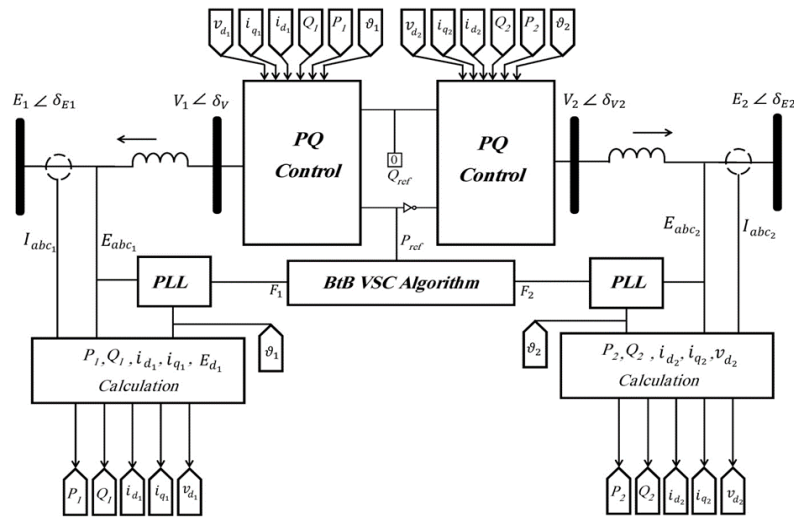

Figure 4. Back-to-back converter control design

3.3. Proposed algorithm for BTB-VSC converter control

The flowchart of the proposed strategy is shown in Figure 5. When the network switches to island mode, the reference frequency of each MG is determined by the interface control scheme converted to its storage devices, according to the battery injection capacity per MG. Local control of the microgrids and the control system of the BTB-VSC converter are managed hierarchically. If the MGs can stabilize their frequency with their sources, the transmission of power from the adjacent MG via the BTB-VSC converter is not necessary. A BTB-VSC converter will be required whenever power outages or oversupply cannot be managed

by local controllers. Therefore, the BTB-VSC control system intervenes and manages the frequency deviation when the frequency value is out of the set points. Power exchange between MGs can be done in one of the following conditions:

− If the first MG has a surplus output which can be realized by 50.002<fl and at the same time the second MG has a shortage of output, ie f2<49.998 in this case the first MG will export power to the second MG It does. The amount of power transmitted in such a state is such that the frequency of each of the MGs reaches the specified value.

− If the second MG has a surplus supply, ie 50. 002<f2 and the first MG has a supply shortage, ie f1<49.998 in this case the second MG transmits power to the first MG. The transfer of power continues until the frequency of each network returns to a steady state and the specified value.

− If none of the above conditions are met, each control system independently controls its sources to keep the frequency within the normal range.
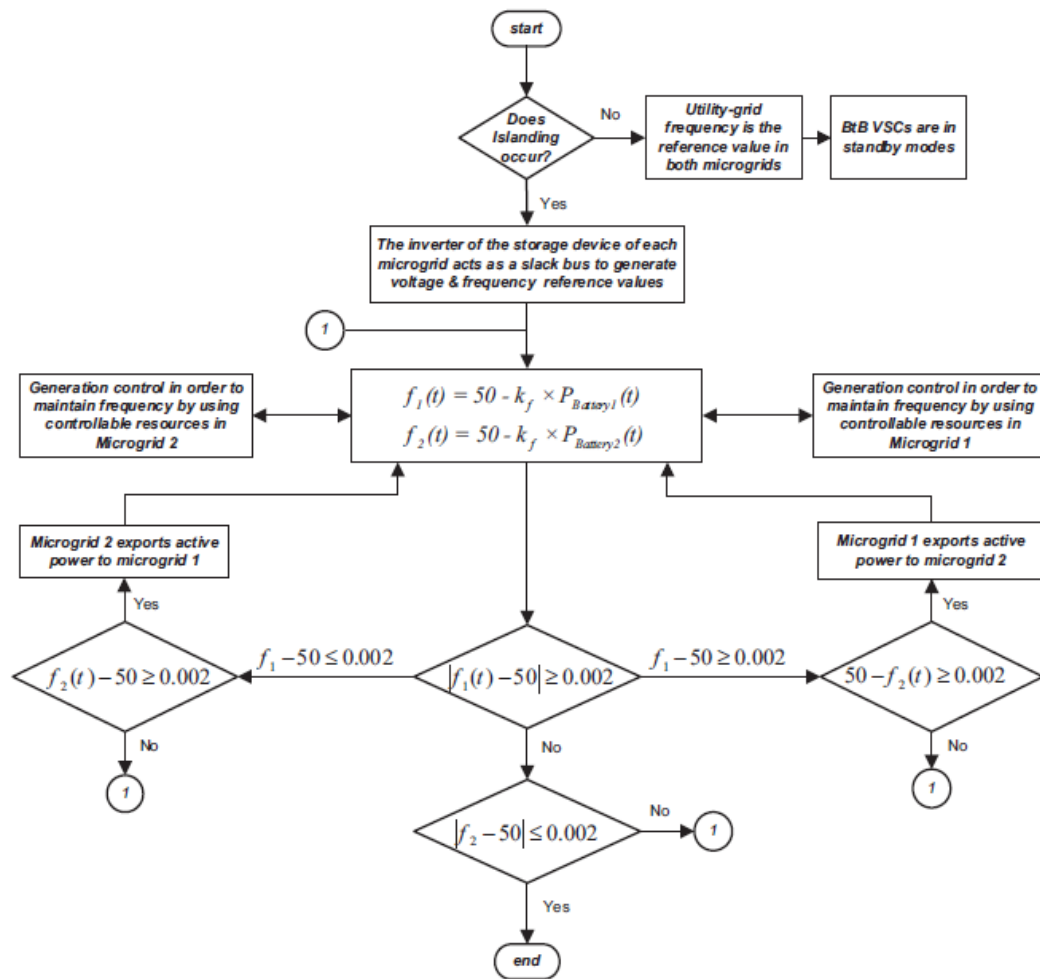

Figure 5. Frequency control algorithm micro flow chart

4. SIMULATION

In the simulation section, the effects of BTB-VSC converter on frequency control are measured in order to measure, validate and evaluate the performance of the proposed model. In the next step, we examine the case where the converter is not in the system and then the two cases are compared. The simulations are performed taking into account the following hypotheses and conditions: i) MGs are fully converter based and transmit all DG resources through MG interfaces; and ii) each MG is able to control locally independently without connecting to the main network in island mode.

Renewable output power is intended to demonstrate the performance of the BTB-VSC static control system. As previously explained, each MG has its own independent control and management system to

maintain the frequency in transient mode, first by interfering with the storage control system by absorbing/injecting force, and secondly by pressing resource-based convert to one. Create a new working point by changing the microgrid reference frequency by the storage device, so neutralize the charge or discharge of the storage device and prepare for the next malfunction of the control [2]. Needless to say, after disconnecting the MGs from the CPU, the local DG controllers do not have enough capacity to maintain the frequency, so a control system is required for each MG storage device for fast response and frequency recovery. However, as low-capacity storage devices, the adjacent microgrid can be useful in this regard and help restore the frequency early on when disruption is initiated by power transmission management via BTB-VSC converters. The dynamic response is investigated and the switching sequence is ignored. Before the island mode occurs, the load of the first MG is set to 5% of its nominal value, so in this mode, the MG injects power into the main network. This means that the first MG overproduces before it goes to island mode. Each microgrid operates at its fixed point before the island state. Before the island state, the second MG is set at 5% of its nominal value, so the second MG has a power shortage that is compensated by the main grid.

Scenario 1: MGs are controlled independently. In this case, the two MGs are controlled completely separately and independently. In addition, each MG uses its own resources to provide its primary and secondary controls well. In this scenario, the local control of each MG is considered and carefully examined. Generally, a MG will be connected to the original grid for most of the time, i.e., performed in the grid-connected mode. In the stand-alone mode, a MG is isolated from the original grid; the highest priority for MGs is to keep a reliable power supply to customers instead of economic benefits. In this stage of the control method, the control of internal and external control loops is used. From the DQ model, it can be seen that when the simultaneous rotation frame DQ is adopted, the flow components are paired with each other. Therefore, to control the active and reactive power independently, i1, 2d and i1, 2q must be separated.

Scenario 2: Two MGs connected by BTB-VSC converter. In scenario 2, the BTB-VSC system establishes a local connection for two microgrids. According to the conditions considered for this scenario, at the moment of the island, the BTB-VSC system must transfer the excess generated power to a network that has a power shortage and if there is a power shortage, it will receive it from another network.

Then the simulation results were evaluated with the presence of BTB-VSC converter and then compared to simulation results in the case where there is no converter. Figure 6 shows that when the island state occurs, there is a frequency disturbance. The first microgrid storage device absorbs excessive power and generates the reference frequency of the microgrid at a value higher than the nominal value.
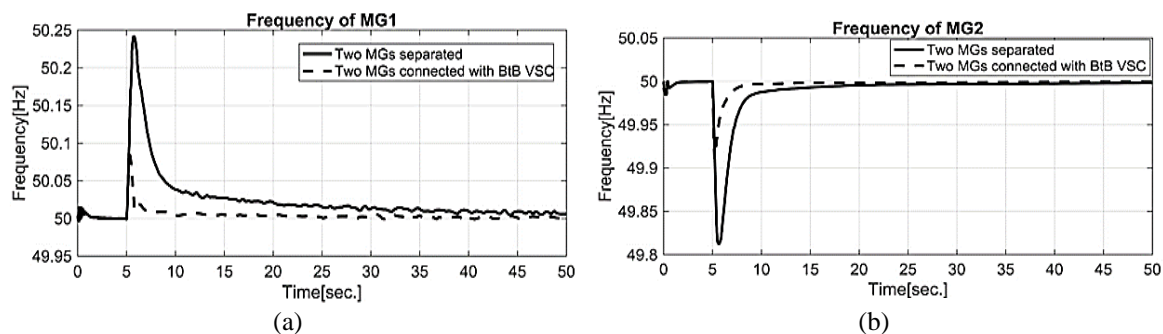

Figure 6. Frequency control algorithm of two interconnected MGs using BTB-VSC converter:
(a) first MG frequency and (b) second MG frequency

At the same time in the second MG, the shortage is compensated by the batteries used as storage device. The MG reference frequency is set to less than 1 Hz. To compensate for the nominal value of the microgrid frequency, according to the proposed algorithm for each separate microgrid, the controlled sources contribute to the frequency control for the output frequency caused by the battery system converter. This process takes several seconds for the controlled sources to change their output power. The reason for this is the slow response of controllable resources.

Scenario 3: Nonlinear stability analysis of MGs connected by BTB-VSC converter. Single-phase ground-to-ground faults are considered to evaluate the performance of two MGs connected by a BTB-VSC converter. Two single-phase faults to ground occur at t=45 and t=65 at two critical points; i) at the bus BTB-VSC converter load point on the second MG and ii) at the interface of the VSC battery converter on the second microgrid.

According to the Figure 7, the injected active power is controlled by the sources. In the case where the two networks are connected by a BTB-VSC converter, in the island mode whenever the MG is overloaded and the second MG is detected, the MG frequency is managed, then, under these conditions, the BTB-VSC 1 control mode of the second power fraction compensates for MG. With too much power the first MGs. As a result, the second MG frequency control is performed satisfactorily and the power loss of the first microgrid is intelligently compensated by the power generating sources.

Figure 7. Active power injected by controllable sources: (a) the first MGs and (b) the second MGs

Figure 8 shows the frequency of MG when single-phase fault occurs in two states without fault and with fault. Frequency change values are shown at T=45 and T=65 seconds. As an error on the second microgrid side, power is extracted from the battery used as the storage source, so the frequency is reduced, but its effect on the output of the converter and the BTB-VSC converter is negligible. This result is due to the interface with PRF control systems, which limits the active and reactive power and thus implicitly and significantly reduces the error effect. At t=65 s, another SLG error occurs at another critical point, so the performance of the BTB-VSC converter is satisfactory and the power generated and transmitted by the BTB-VSC converter is not affected. The following figure shows the output capacities of MG types with similar errors in the second MG.

Figure 9 shows the output capacities of different MGs during the same errors in the second MG, as clearly shown in the figure, that the outputs of the first MG (intact) do not have a definite effect of error in the second MG; Defective MG output capacities are now reduced due to battery intervention to improve the system. For BTB converters, all equilibrium points in the system constitute an area called the operating region. Operating region specifies the reactive and active power for BTB converters in both supply and absorbs modes. With the gradual increase in rankings and the decrease in semiconductor technology losses in recent years, the idea of making full use of the potential of the BTB-VSC converter for active and reactive power management is possible with the appropriate control law. BTB converter uses multi-level topologies to increase operating voltage levels. The operating region creates valid combinations for both P and Q for the performance of the BTB converter, so the choice of P and Q must be based on principles and rules because both must be within the operating range defined by the operating parameters. In this research, a nonlinear control algorithm in the operational area is proposed to control BTB-VSC converters. Proper implementation of control strategy in case of errors and dynamic behaviors is the main motivation of this design. For this purpose, at least one of the VSCs is used to control the DC voltage lines and the other to control the active power. As a result, the active power is automatically balanced between the VSCs.
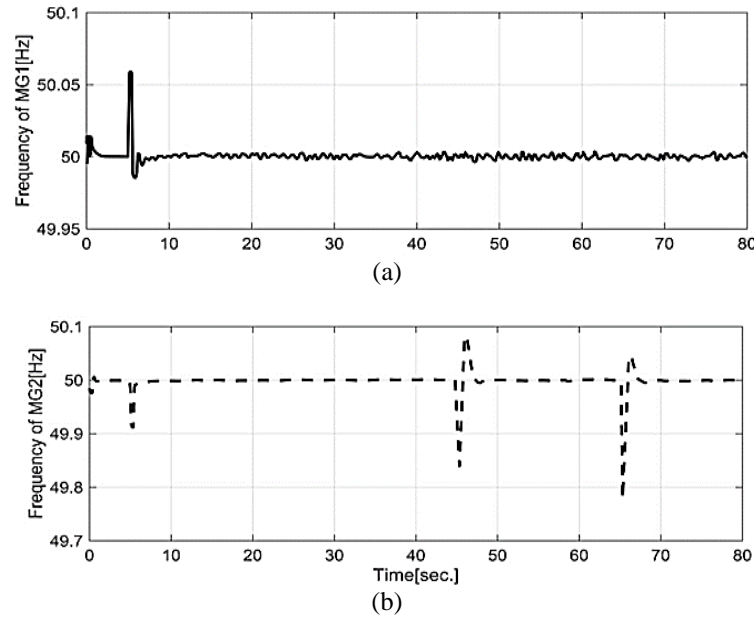
(a)

(b)

Figure 8. MG frequency when single-phase fault occurs on the ground in the first MG: (a) frequency of the first (healthy) MG without any trace of error and (b) second MG frequency (error)
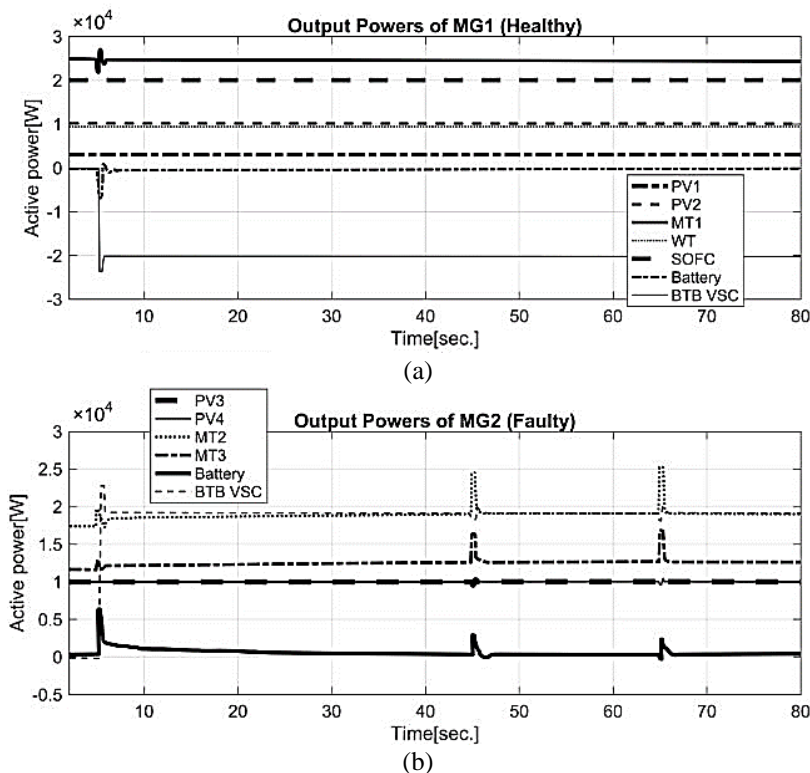

(a)

(b)

Figure 9. Microgrid output power when a single-phase fault occurs on the ground in the first microgrid: (a) the first (healthy) microgrid output power does not show any clear effect of error occurring on the other microgrid and (b) second (malfunctioning) MG output with battery intervention to improve the system

4.   CONCLUSION

In order to compare the scenarios with each other, as the results have shown, for the one and two scenarios, when the MGs operate independently and when connected by a BTB converter, the MGs they are

separated from the main network and are in a new frequency mode. As shown in the results, it shows injectable active power by controlled sources. In cases where the two networks are connected by BTB-VSC converter, in island mode whenever the MG overloads and the second MG is detected, the MG frequency is then managed, then, under these conditions, The BTB-VSC 1 control mode compensates for the second MG power deficit by over-powering the first micro channel. As a result, both the second MG frequency is controlled and has a satisfactory performance, and the power loss of the first microgrid is compensated by its controllable sources and the network maintains its stability. But in the third scenario, the stability conditions of the system under single-phase error in two points of the system are investigated. The results showed that the stability of the MGs was at fault.

REFERENCES

[1] Sathyaprabakaran B, S. Paul, and D. Chatterjee, "A New strategy for on- line Droop adjustment for Microgrid connected DGs," *International Journal of Power Electronics and Drive Systems (IJPEDS),* vol 9, no 1, 2018, doi: 10.11591/ijpeds.v9.i1.pp139-149.
[2] B. P. Ganthia, V. Agarwal, K. Rout and M. K. Pardhe, "Optimal control study in DFIG based wind energy conversion system using PI & GA," 2017 *International Conference on Power and Embedded Drive Control (ICPEDC)*, 2017, pp. 343-347, doi: 10.1109/ICPEDC.2017.8081112.
[3] A. M. R. Lede, M. G. Molina, M. Martinez and P. E. Mercado, "Microgrid architectures for distributed generation: A brief review," 2017 *IEEE PES Innovative Smart Grid Technologies Conference - Latin America (ISGT Latin America)*, 2017, pp. 1-6, doi: 10.1109/ISGT-LA.2017.8126746.
[4] R. Bayindir, E. Hossain, E. Kabalci, and R. Perez "A comprehensive study on microgrid technology," *International Journal of Renewable Energy Research (IJRER)*, vol. 4, no. 4, pp. 1094-1107, 2014, doi: 10.20508/ijrer.v4i4.2005.g6455.
[5] L. F. N. Delboni, D. Marujo, P. P. Balestrassi, and D. Q. Oliveira, *Electrical power systems: evolution from traditional configuration to distributed generation and microgrids*, Microgrids Design and Implementation. Springer, Cham, Nov. 2018, pp. 1-25, doi: 10.1007/978-3-319-98687-6_1
[6] E. Afshari *et al.*, "Control strategy for three-phase grid-connected PV inverters enabling current limitation under unbalanced faults," in *IEEE Transactions on Industrial Electronics*, vol. 64, no. 11, pp. 8908-8918, Nov. 2017, doi: 10.1109/TIE.2017.2733481.
[7] C. Wouters, "Towards a regulatory framework for microgrids—The Singapore experience," *Sustainable Cities and Society*, vol. 15, pp. 22-32, 2015, doi: 10.1016/j.scs.2014.10.007.
[8] M. Soshinskaya, W.H.J. Crijns-Graus, J. M. Guerrero, and J. C. Vasquez, "Microgrids: Experiences, barriers and success factors," *Renewable and Sustainable Energy Reviews*, vol. 40, no 1, pp. 659-672, Dec 2014, doi: 10.1016/j.rser.2014.07.198.
[9] M. Warneryd, M. Håkansson, and K. Karltorp, "Unpacking the complexity of community microgrids: A review of institutions' roles for development of microgrids," *Renewable and Sustainable Energy Reviews*, vol .121, pp. 659-672, Apr 2020, doi: 10.1016/j.rser.2019.109690.
[10] A. O. Erick and K. A. Folly, "Reinforcement learning approaches to power management in grid-tied microgrids: a review," *2020 Clemson University Power Systems Conference (PSC)*, 2020, pp. 1-6, doi: 10.1109/PSC50246.2020.9131138.
[11] E. M. Khawla, C. Dhia and S. Lassaad, "LVRT control strategy for three-phase grid connected PV systems," *2017 International Conference on Green Energy Conversion Systems (GECS)*, 2017, pp. 1-7, doi: 10.1109/GECS.2017.8066237.
[12] A. C. Luna, N. L. Diaz, M. Graells, J. C. Vasquez and J. M. Guerrero, "Mixed-integer-linear-programming-based energy management system for hybrid PV-wind-battery microgrids: modeling, design, and experimental verification," in *IEEE Transactions on Power Electronics*, vol. 32, no. 4, pp. 2769-2783, April 2017, doi: 10.1109/TPEL.2016.2581021.
[13] J. Zhou, F. Tang, Z. Xin, S. Huang, P. C. Loh and J. Jiang, "Differences between continuous single-phase and online three-phase power-decoupled converters," in *IEEE Transactions on Power Electronics*, vol. 34, no. 4, pp. 3487-3503, April 2019, doi: 10.1109/TPEL.2018.2856830.
[14] S. Chandak, and P.K. Rout, "The implementation framework of a microgrid: A review," *International Journal of Energy Research*, vol. 45, no. 1, Oct 2020, doi: 10.1002/er.6064.
[15] Z. Shahbazi, A. Ahmadi, A. Karimi and Q. Shafiee, "Performance and vulnerability of distributed secondary control of AC microgrids under cyber-attack," *2021 7th International Conference on Control, Instrumentation and Automation (ICCIA)*, 2021, pp. 1-6, doi: 10.1109/ICCIA52082.2021.9403548.
[16] T. Wang, J. Qiu, S. Fu and W. Ji, "Distributed fuzzy H_{∞} filtering for nonlinear multirate networked double-layer industrial processes," in *IEEE Transactions on Industrial Electronics,* vol. 64, no. 6, pp. 5203-5211, June 2017, doi: 10.1109/TIE.2016.2622234.
[17] C. Dou, Z. Zhang, D. Yue and Y. Zheng, "MAS-based hierarchical distributed coordinate control strategy of virtual power source voltage in low-voltage microgrid," in *IEEE Access*, vol. 5, pp. 11381-11390, 2017, doi: 10.1109/ACCESS.2017.2717493.
[18] N. M. Dehkordi, N. Sadati and M. Hamzeh, "Distributed robust finite-time secondary voltage and frequency control of islanded microgrids," in *IEEE Transactions on Power Systems*, vol. 32, no. 5, pp. 3648-3659, Sept. 2017, doi: 10.1109/TPWRS.2016.2634085.
[19] N. M. Dehkordi, N. Sadati and M. Hamzeh, "Fully distributed cooperative secondary frequency and voltage control of islanded microgrids," in *IEEE Transactions on Energy Conversion*, vol. 32, no. 2, pp. 675-685, June 2017, doi: 10.1109/TEC.2016.2638858.
[20] D. O. Amoateng, M. Al Hosani, M. S. Elmoursi, K. Turitsyn and J. L. Kirtley, "Adaptive voltage and frequency control of islanded multi-microgrids," in *IEEE Transactions on Power Systems*, vol. 33, no. 4, pp. 4454-4465, July 2018, doi: 10.1109/TPWRS.2017.2780986.
[21] Q. Shafiee, J. M. Guerrero and J. C. Vasquez, "Distributed secondary control for islanded microgrids—a novel approach," in *IEEE Transactions on Power Electronics*, vol. 29, no. 2, pp. 1018-1031, Feb. 2014, doi: 10.1109/TPEL.2013.2259506.
[22] U. Sowmmiya and U. Govindarajan, "Control and power transfer operation of WRIG-based WECS in a hybrid AC/DC microgrid," *IET Renewable Power Generation*, vol. 12, no. 3, pp. 359-373, Feb. 2018, doi: 10.1049/iet-rpg.2017.0298.
[23] Z. Zhang *et al.*, "An event-triggered secondary control strategy with network delay in islanded microgrids," in *IEEE Systems Journal*, vol. 13, no. 2, pp. 1851-1860, June 2019, doi: 10.1109/JSYST.2018.2832065.
[24] J. He and Y. W. Li, "An enhanced microgrid load demand sharing strategy," in *IEEE Transactions on Power Electronics*, vol. 27, no. 9, pp. 3984-3995, Sept. 2012, doi: 10.1109/TPEL.2012.2190099.

[25] N. Kumar, B. Singh and B. K. Panigrahi, "Integration of solar PV with low-voltage weak grid system: using maximize-m Kalman filter and self-tuned P&O algorithm," in *IEEE Transactions on Industrial Electronics*, vol. 66, no. 11, pp. 9013-9022, Nov. 2019, doi: 10.1109/TIE.2018.2889617.

[26] A.K. Roy, P. Basak, and G.R. Biswal, "Low voltage ride through capability enhancement in a grid-connected wind/fuel cell hybrid system via combined feed-forward and fuzzy logic control," *IET Generation, Transmission & Distribution*, vol. 13, no. 13, pp. 2866-2867, Jul 2019, doi: 10.1049/iet-gtd.2019.0021.

[27] F. Tang, J. Zhou, Z. Xin, S. Huang and P. C. Loh, "An improved three-phase voltage source converter with high-performance operation under unbalanced conditions," in *IEEE Access*, vol. 6, pp. 15908-15918, 2018, doi: 10.1109/ACCESS.2018.2814200.

[28] P. Khamphakdi, M. Nitta, M. Hagiwara and H. Akagi, "Zero-voltage ride-through capability of a transformerless back-to-back system using modular multilevel cascade converters for power distribution systems," in *IEEE Transactions on Power Electronics*, vol. 31, no. 4, pp. 2730-2741, April 2016, doi: 10.1109/TPEL.2015.2445379.

[29] A. Chauhan, and R.P. Saini, "A review on integrated renewable energy system based power generation for stand-alone applications: configurations, storage options, sizing methodologies and control," *Renewable and Sustainable Energy Reviews*, vol. 38 , pp. 99-120, Oct 2014, doi: 10.1016/j.rser.2014.05.079.

[30] C. X. Rosero, M. Velasco, P. Martí, A. Camacho, J. Miret and M. Castilla, "Active power sharing and frequency regulation in droop-free control for islanded microgrids under electrical and communication failures," in *IEEE Transactions on Industrial Electronics*, vol. 67, no. 8, pp. 6461-6472, Aug. 2020, doi: 10.1109/TIE.2019.2939959.

[31] Z. Zhang, D. Chunxia, Y. Dong, Z. Bo, and L. Wei, "A decentralized control method for frequency restoration and accurate reactive power sharing in islanded microgrids," *Journal of the Franklin Institute*, vol. 355 , pp. 8874-8890, Nov 2018, doi: 10.1016/j.jfranklin.2018.09.024.

[32] A. Husna, M. Roslan, and M. Mat, "Droop control technique for equal power sharing in islanded microgrid," *International Journal of Power Electronics and Drive Systems (IJPEDS)*, vol. 10, no. 1, pp. 530-537, March 2019, dx.doi.org/10.11591/ijpeds.v10.i1.pp530-537.

BIOGRAPHIES OF AUTHORS

Mostafa Abbasi 🆔 👤 sc ⊙ was born on 4 April 1987 in Lamard. He received his bachelor's and master's degrees in electrical engineering from IAU Bushehr University, Bushehr, Iran and IAU Najaf Abad, Isfahan, Iran, respectively, in 2009 and 2013 and graduated with first class honors. He is currently a PhD student in power engineering. He is the author of more than 30 journal and conference papers. His teaching and research interests include power systems and transient transformers, production development planning, and microgrid systems. He can be contacted at email: mostafa.abbasi@miau.ac.ir.

Mehdi Nafar 🆔 👤 sc ⊙ was born on April 24, 1979 in Marvdasht, Iran. He received his BS, MS and Ph.D. degrees in electrical engineering in 2002, 2004 and 2011 from PWIT University, Tehran, Iran and Amirkabir University of Technology (AUT), Tehran, Iran and Islamic Azad University, Science and research Branch, Tehran, Iran, respectively, graduating all with First Class Honors. He is an assistant professor of Electrical Engineering Department, Marvdasht Branch, Islamic Azad University, Marvdasht, Iran. He is the author of more than 50 journal and conference papers. His teaching and research interest include power system and transformers transients, lightening protection and optimization methods in power systems. He can be contacted at email: mnafar@miau.ac.ir.

Mohsen Simab 🆔 👤 sc ⊙ received the BSc degree in Electrical Engineering from Amir Kabir University, Tehran, Iran, and the MSc and PhD degrees from Tarbiat Modares University, Tehran, Iran, in 2004, 2006, and 2011, respectively. He is an Assistant Professor in power systems at the Department of Electrical Engineering, Marvdasht Branch, Islamic Azad University, Marvdasht, Iran. His main research interests are electric distribution regulation, power system operation, and power system reliability. He can be contacted at email: msimab@miau.ac.ir.